Sawmill Residue Valorization as Adsorbent for Cd²⁺ from Aqueous Solution

Ali El-Rayyes,^{a,b} Ibrahim Arogundade,^{c,*} Ezekiel Folorunsho Sodiya,^c Edwin Andrew Ofudje,^c Moamen S. Refat,^d Amnah Mohammed Alsuhaibani,^e and James Asamu Akande ^f

Raw sawmill wood adsorbent (RSWA) and sawmill wood biochar adsorbent (SWBA) were evaluated as eco-friendly materials for removing cadmium ions (Cd2+) from aqueous solutions. The sawmill waste was thermally treated, and the resulting biochar was characterized using FT-IR, SEM, and BET analyses, revealing a rough, porous structure comprising functional groups that enhance adsorption. Batch adsorption experiments demonstrated that SWBA exhibited a higher adsorption capacity (85.4 mg/g at 45 °C) compared to RSWA (78.6 mg/g at 40 °C), with equilibrium times of 180 min for SWBA and 150 min for RSWA. Adsorption efficiency was pH-dependent, with optimal removal occurring at pH 6 for SWBA and pH 5 for RSWA. Kinetic modeling confirmed that adsorption followed the pseudo-second-order model, while isotherm studies indicated a stronger correlation with the Freundlich model. Thermodynamic analysis confirmed the process to be endothermic and spontaneous. Desorption studies revealed a decline in adsorption efficiency over multiple cycles, with RSWA exhibiting slightly better desorption performance than SWBA. These findings highlight sawmill wood biochar as a cost-effective and sustainable solution for wastewater treatment, particularly in heavy metal removal.

DOI: 10.15376/biores.20.3.7048-7074

Keywords: Adsorbent; Biochar; Pollution; Sawmill waste; Valorization

Contact information: a: Center for Scientific Research and Entrepreneurship, Northern Border University, Arar 73213, Saudi Arabia; b: Chemistry Department, College of Science, Northern Border University, Arar, Saudi Arabia; c: Department of Chemical Sciences, Mountain Top University, Ogun State, Nigeria; d: Department of Chemistry, College of Science, Taif University, P.O. Box 11099, Taif 21944, Saudi Arabia; e: Department of Sports Health, College of Sport Sciences & Physical Activity, Princess Nourah bint Abdulrahman University, P.O. Box 84428, Riyadh 11671, Saudi Arabia; f: Department of Chemistry and Biochemistry, Caleb University, Imota, Lagos State, Nigeria;

* Corresponding author: ibrahimadearogundade@gmail.com

INTRODUCTION

One of the most essential resources that sustains life, supports ecosystems, and drives economic activities is water. It plays a critical role in agriculture, industry, and domestic use, serving as a fundamental component for food production, energy generation, and sanitation. Clean water is vital for human health, as it prevents waterborne diseases and ensures proper hydration and hygiene (Ofudje *et al.* 2022a). Additionally, aquatic ecosystems rely on unpolluted water to maintain biodiversity, as rivers, lakes, and oceans provide habitats for countless species. However, water contamination has become a major environmental challenge due to the discharge of industrial, agricultural, and domestic pollutants into water bodies (Ahmad and Hameed

2010; Adeogun *et al.* 2012). The rapid industrialization and expansion of manufacturing activities have increased the prevalence of toxic heavy metals in wastewater, posing significant risks to environmental and human health (Ahmad and Hameed 2010; Adeogun *et al.* 2012). Among these pollutants, cadmium ions (Cd²+) are widely used in industries such as batteries, electroplating, metal coatings, pigments in plastics and ceramics, stabilizers in PVC products, and electronic components including solar panels and semiconductors (Crini and Badot 2008; Khan *et al.* 2017; Leila *et al.* 2022; Ngeno *et al.* 2022; Surjani *et al.* 2023). Industrial activities, including mining, smelting, electroplating, and battery manufacturing, release Cd²+ into the environment, contributing to water contamination and the spread of toxic chemicals (Crini and Badot 2008; Khan *et al.* 2017; Leila *et al.* 2022; Ngeno *et al.* 2022; Surjani *et al.* 2023).

Cadmium could also accumulate in soil through phosphate fertilizers and sewage sludge. In addition, E-waste, incineration, and landfill leachate contribute to cadmium pollution (Khan *et al.* 2017; Leila *et al.* 2022; Surjani *et al.* 2023). Toxicity to living organisms could arise from its propensity to bioaccumulate in plants, animals, and humans, causing kidney damage, bone fractures, and carcinogenic effects (Leila *et al.* 2022; Surjani *et al.* 2023). Thus, cadmium (Cd²+) poses serious environmental and health risks and effective pollution control measures, including the use of simple and advanced remediation technologies and sustainable industrial practices, are necessary to mitigate their harmful impacts (Henao-Toro *et al.* 2024).

Conventional water treatment methods, such as ion exchange, membrane filtration, chemical precipitation are often costly and generate secondary waste, driving the need for more sustainable and low-cost alternatives (Gupta and Suhas 2009; Ofudje *et al.* 2020b). In response, researchers have turned to valorizing biomass waste, including sawmill wood, as eco-friendly adsorbents for removing contaminants from water sources (Bhatnagar and Sillanpää 2010; Qiu *et al.* 2021, 2022). These materials are cheap, readily available and possess rich structures with various functional groups that can be explored for the uptake of contaminants. The increasing demand for efficient and sustainable water treatment methods has led researchers to explore various waste materials as potential adsorbents for dyes and heavy metals in wastewater.

Sawmill wood residues, a renewable and abundant byproduct of the wood processing industry, has shown potential as an adsorbent because of its functional groups and natural porosity, which allow it to capture both heavy metals and dyes from aqueous solutions (Šćiban et al. 2004, Kayode et al. 2022). Sawmill wood, especially when carbonized or chemically modified, possesses functional groups such as hydroxyl, carboxyl, and phenolic groups, which enhance its capacity to adsorb both organic and inorganic contaminants (Šćiban et al. 2004; Dutta et al. 2021; Kayode et al. 2022; Dutta et al. 2023). While sawmill waste (such as sawdust, wood shavings, and wood chips) has potential as a low-cost adsorbent for pollutants, literature reports indicate several major challenges such as low adsorption efficiency due to limited surface area, insufficient functional groups that enhance adsorption capacity, and poor mechanical stability causing it to easily degraded in water and can break down into fine particles, leading to clogging in filtration systems (Daiana et al. 2022; Akrivi et al. 2025). Also, some raw sawmill waste can contain leachable organic compounds that may cause secondary pollution (Daiana et al. 2022). Valorization, which refers to the process of upgrading sawmill waste to improve its adsorption capabilities and commercial value via heat treatment, offers some key benefits that include enhanced adsorption efficiency as a result of increase surface area and creation of more adsorption sites for pollutants. In addition, the

improved structural stability caused by the compaction strengthens the material, thus preventing breakdown and clogging in water treatment systems. Instead of being burned or discarded, sawmill waste is converted into a valuable product, thereby reducing its environmental impact. Such materials can be used to adsorb several pollutants such as heavy metals (Cd²⁺, Pb²⁺, Cr⁶⁺), dyes (malachite green, methylene blue), and organic contaminants (Daiana *et al.* 2022; Akrivi *et al.* 2025; Fernández-Sosa *et al.* 2025). The porosity and surface chemistry of sawmill wood make it suitable for binding positively charged ions such as Cd²⁺ and cationic dyes including malachite green, which are prevalent contaminants in industrial wastewater.

Regeneration is a critical factor in evaluating the effectiveness and reusability of an adsorbent. Common regeneration techniques include chemical regeneration, thermal regeneration, microwave-assisted regeneration, electrochemical regeneration, and ultrasound regeneration (Lata *et al.* 2015; Alsawy *et al.* 2022). Acids such as HCl and alkalis such as NaOH solutions have been reported to have disrupted ionic or coordination bonds between adsorbates and adsorbents, facilitating desorption through ion exchange or dissolution of surface precipitates.

This work explored the potential of sawmill wood biochar as sorbent for the adsorption of Cd²⁺ and investigating its adsorption mechanisms, efficiency under various conditions, and economic and environmental advantages in comparison to conventional methods. This approach not only addresses the issue of sawmill waste disposal but also contributes to the development of a circular economy, where waste products are repurposed for environmental applications.

MATERIALS AND METHODS

Materials

The cadmium salt (CdSO₄) and other chemicals used in this study were purchased from Aldrich Sigma, India and used without further purification. All glassware were thoroughly washed with distilled water, and dried.

Preparation and Modification of Sawmill Wood Adsorbent

The sawmill wood waste was collected from a wood factory in Pakoto, Ogun State, Nigeria, cleaned, and dried to remove any impurities or residual moisture. To enhance the adsorbent's properties, thermal treatment method was employed in which the dried samples were fed into a furnace and heated to a temperature of 700 °C for 3 h. The carbonized wood product was then removed from the furnace, allowed to cool to room temperature and ground to a uniform particle size to ensure consistent adsorption characteristics. The sawmill wood biochar adsorbent (SWBA) was kept in an airtight bag for further characterization.

Characterization of the Sawmill Wood Adsorbent

The prepared adsorbent was examined using some techniques to understand its physical and chemical properties, which are crucial for determining adsorption efficiency. Fourier transform infrared (FT-IR, Shimadzu 8400S FT-IR instrument, Japan) spectroscopy was used to identify the functional groups that facilitate contaminant binding through the transmission mode, with KBr pellet preparation. Scanning electron microscopy (SEM) was used to assess the surface morphology and porosity (SEM

Phenom ProX, Thermo Fisher Scientific, USA), while Brunauer–Emmett–Teller (BET, Quantachrome corporation, NOVA 4000e 1 BET machine, Anton Paar USA) analysis provided insights into surface area and pore size distribution, which are important factors for adsorption efficiency. The thermal behavior of the adsorbent was investigated using thermographic analyzer (TGA 4000, Perkin Elmer, Netherlands). The bulk density, pore size, pore volume, and surface area of the sawmill wood waste were measured using a Quantachrome NOVA 2200C (USA), while the zero-point charge (pHaaZPC) of the adsorbent was determined using a Zetasizer Nano ZS analyzer (Malvern, UK).

Adsorption Studies

Adsorption experiments (batch process) were done to assess the adsorption capacities of sawmill wood for Cd²+ ions. Approximately 20 mg of the adsorbent was added to aqueous solutions containing known concentrations of Cd²+ in several conical flasks, and the mixture was agitated at a constant speed of 150 rpm to ensure homogeneity on orbital shaker. Key variables such as initial concentration of Cd²+, adsorbent dosage, contact time, pH, and temperature were varied to determine their effect on adsorption capacity. The optimal pH was adjusted for each pollutant. At different time interval, small amount of the contaminant was removed, and analyzed by atomic absorption spectroscopy (AAS) (iCETM 3500, Thermo Fisher Scientific, Waltham, MA, USA). The removal amount and the percentage removal were computed using Eqs. 1 and 2:

Amount adsorbed,
$$Q_e = \frac{C_o - C_e}{m}V$$
 (1)

Percentage Removal
$${}^{6}Q_{e} = \frac{C_{o} - C_{e}}{C_{o}} \times 100$$
 (2)

 C_0 and C_e are the amount of Cd^{2+} available at the beginning and at equilibrium, V is the solution volume (L), and m is the mass of the adsorbent (mg).

Regeneration Evaluation

Regeneration experiments were done so as to assess the reusability of sawmill wood as an adsorbent. After each adsorption cycle, the sawmill wood was desorbed using different eluents (water, ethanol, HCl, acetic acid, and NaOH), to remove the adsorbed Cd²⁺. The adsorbent was then washed and reused in subsequent adsorption cycles to determine its long-term stability and cost-effectiveness. The mixture was separated, and the contents left was analyzed by AAS method (iCETM 3500, Thermo Fisher Scientific, Waltham, MA, USA). This procedure was repeated for five cycles, following the same experimental protocol, and the percentage desorption (PD) was calculated using Eq. 3 below,

$$PD(\%) = \frac{AD}{AA}X100\tag{3}$$

where AD is the desorbed amount of Cd^{2+} amount (mg), and Cd^{2+} amount (mg) adsorbed is denoted as AA. Each experiment was done in triplicate, and the average values were recorded.

RESULTS AND DISCUSSION

Characterizations

The FT-IR spectra provide evidence of the chemical functional groups present in sawmill wood biochar before (a) and after (b) adsorption (Fig. 1). The peak around 3200 to 3500 cm⁻¹ is associated with hydroxyl (-OH) groups from cellulose, lignin, or adsorbed water (Kayode *et al.* 2022; Abewaa *et al.* 2023). An increase in intensity after adsorption suggests the interaction between the hydroxyl groups and the adsorbed contaminants. The peaks around 1685 to 1705 cm⁻¹ corresponds to C=O or C=C stretchings (Kayode *et al.* 2022; Abewaa *et al.* 2023). The changes in intensity or shifts in this region suggest complexation between pollutant and carbonyl functional groups. The presence of the SO₃-group was confirmed with a peak at 1165 cm⁻¹, where the appearance of peaks at 1033 and 1015 cm⁻¹ suggest the presence of O–S–O or C-O stretchings (Wang *et al.* 2011; Hasan *et al.* 2012). The presence of increased peak intensity at 550 cm⁻¹ indicates the formation of metal-ligand bonds, confirming the adsorption of Cd²⁺. The significant differences between the two spectra indicate that adsorption of contaminants has altered the functional groups on the biochar surface.

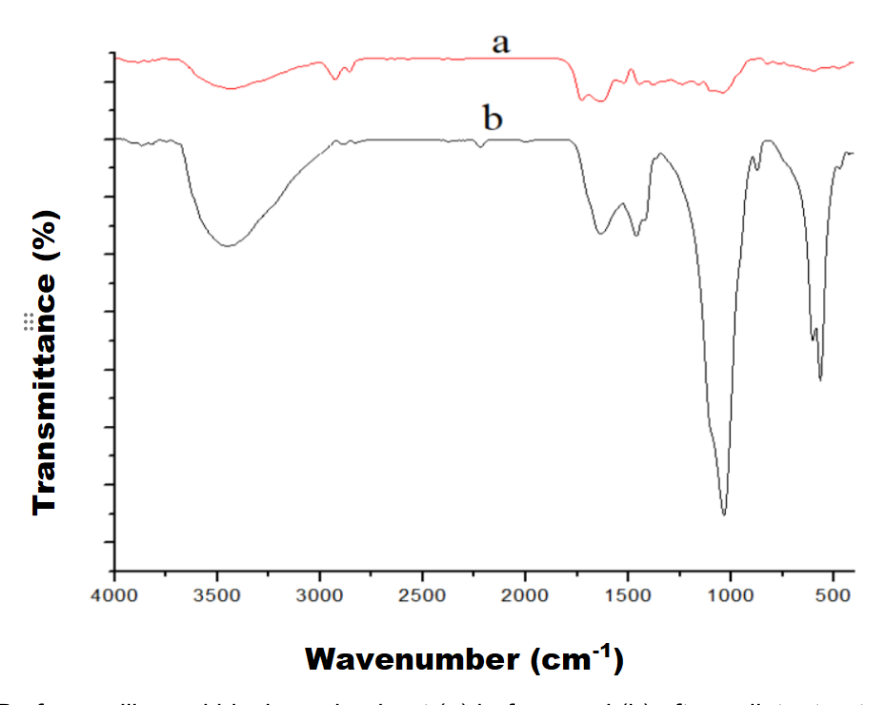


Fig. 1. FTIR of sawmill wood biochar adsorbent (a) before, and (b) after pollutant uptake

The SEM images illustrate the morphological changes in sawmill wood biochar before (a) and after (b) adsorption of Cd²⁺ ions, as shown in Fig. 2. These microstructural variations provide insight into the adsorption efficiency and surface interactions between the adsorbent and the heavy metal ions. The surface morphology before adsorption (Fig. 2a), the surface of the valorized wood mill waste appears rough, porous, and uneven, with a significant number of cavities and irregular structures. The observed porosity suggests a high surface area, which is essential for effective adsorption. A high surface area also would be consistent with the presence of numerous functional groups that may facilitate metal ion binding through mechanisms such as ion exchange, electrostatic attraction, or complexation. The surface morphology after adsorption (Fig. 2b), in contract reveals a

smoother, denser, and more compact surface, with a reduction in visible pores and cavities. The reduction in roughness and porosity further indicates that the adsorption process may have resulted in pore blockage and structural compaction, which are common after successful metal ion adsorption.

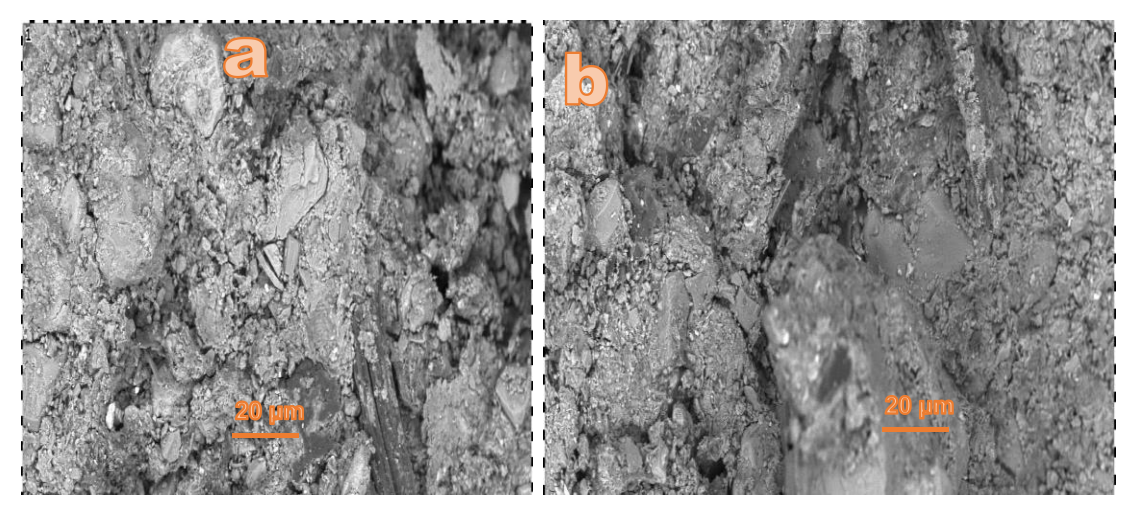


Fig. 2. SEM of biochar adsorbent (a) before, and (b) after pollutant uptake

The physicochemical characteristics of an adsorbent play a crucial role in determining its adsorption capacity, efficiency, and suitability for pollutant removal. The comparison of raw sawmill wood adsorbent (RSWA) and sawmill wood biochar adsorbent (SWBA) highlights the impact of biochar treatment on key adsorption properties, including surface area, pore volume, pore size, and bulk density, as presented in Table 1. The surface area increased from 102.0 m²/g for RSWA to 195.1 m²/g for SWBA, representing a 91.2% enhancement. This significant increase can be attributed to the pyrolysis process, which promotes the development of additional micropores and enhances the adsorbent's porous structure, thereby improving its overall adsorption capacity. This expanded surface area creates additional active sites for adsorption, enhancing the adsorbent's efficiency in capturing contaminants (Henao-Toro et al. 2024). Similarly, the pore volume of SWBA (0.29 cm²/g) was slightly higher than that of RSWA (0.26 cm²/g), suggesting an improved porosity that further enhances the adsorptive potential. The average pore size of SWBA (2.47 nm) was slightly larger than that of RSWA (2.32 nm), indicating that biochar treatment contributed to minor structural modifications that allow for better accessibility of adsorbate molecules. Since both adsorbents have pore sizes within the range 2 to 50 nm, which is in the range of mesopores, they are well-suited for adsorbing organic pollutants and heavy metal ions from wastewater. The bulk density of SWBA (0.235 g/cm²) is slightly higher than that of RSWA (0.218 g/cm²), implying that biochar treatment increases the material's compactness. This increase may enhance handling and packing efficiency in practical adsorption applications, such as column-based filtration systems.

Parameters	RSWA	SWBA
Surface area (m²/g)	102.04	195.14
Pore volume (cm ² /g)	0.26	0.29
Average pore Size (nm)	2.32	2.47
Bulk density (g/cm²)	0.218	0.235
pH _{ZPC}	4.25	4.51

Table 1. Physicochemical Features of the Sawmill Wood Waste

The thermogravimetric analysis plot represents the thermal degradation behavior of sawmill wood waste under increasing temperature conditions, as shown in Fig. 3. A slight drop in weight at around 30 to 130 °C is likely due to the evaporation of moisture and volatile compounds (Guida *et al.* 2019; Khan *et al.* 2021). A significant weight loss occurred in the range of 250 to 500 °C, indicating the breakdown of major wood components as hemicellulose degradation (220 to 330 °C), decomposition of cellulose (320 to 403 °C), and lignin degradation (300 to 500 °C, broader range) (Guida *et al.* 2019; Khan *et al.* 2021). This is the primary pyrolysis phase. Beyond 500 °C, weight loss slowed significantly, and this suggests the formation of char and carbonaceous residue, which slowly degrades at higher temperatures (Guida *et al.* 2019; Khan *et al.* 2021). The sharp weight loss confirms the presence of cellulose and hemicellulose, typical for biomass materials. The residual weight (less than 10%) suggests the presence of inorganic ash content from minerals or impurities in the wood waste. The decomposition pattern aligns with typical thermal behavior of lignocellulosic biomass.

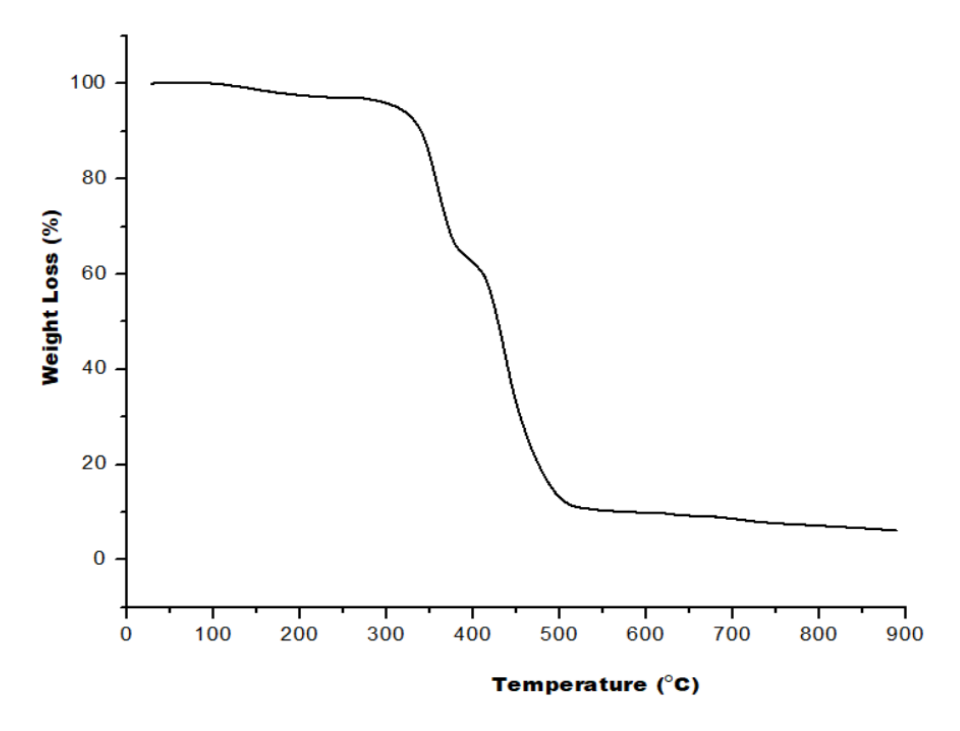


Fig. 3. TGA of sawmill wood adsorbent.

Influence of Operational Parameters

Time and initial pollutants concentrations effects

The adsorption data in Figs. 4 and 5 show how time and initial cadmium ion concentration impacted the adsorption capacity of the sawmill wood adsorbents. For RSWA (Fig. 4), rapid adsorption occurred within the first 90 to 150 min, followed by a slower increase as equilibrium was approached. Higher initial concentrations (30 to 180 mg/L) enhanced adsorption due to a stronger driving force for mass transfer (Akinhanmi *et al.* 2020; Ofudje *et al.* 2020b). For SWBA (Fig. 5), adsorption increased within 120 to 150 min, reaching equilibrium at 180 min with no further significant uptake. Higher cadmium concentrations also increased adsorption, peaking at 67.3 mg/g at 180 mg/L, though the rate of increase slowed as saturation approached (Ofudje *et al.* 2020b). The differences in adsorption efficiency between RSWA and SWBA may be due to variations in surface area, with valorized samples exhibiting larger surface areas.

The longer equilibrium time observed for sawmill wood biochar adsorbent (SWBA), despite its higher adsorption capacity compared to raw sawmill wood adsorbent (RSWA), can be attributed to differences in pore structure, surface area distribution, and surface chemistry. RSWA, being a raw lignocellulosic material, retains a more complex, less uniform surface structure and a higher proportion of macropores and mesopores, which may impede rapid diffusion of adsorbate molecules. Additionally, the absence of thermal modification means that surface functional groups are less organized and potentially more heterogeneous, contributing to slower kinetics due to variable binding site energies and accessibility. In contrast, SWBA undergoes pyrolysis, which enhances pore development (particularly micropores) and increases surface uniformity, thereby facilitating faster intraparticle diffusion and external mass transfer rates.

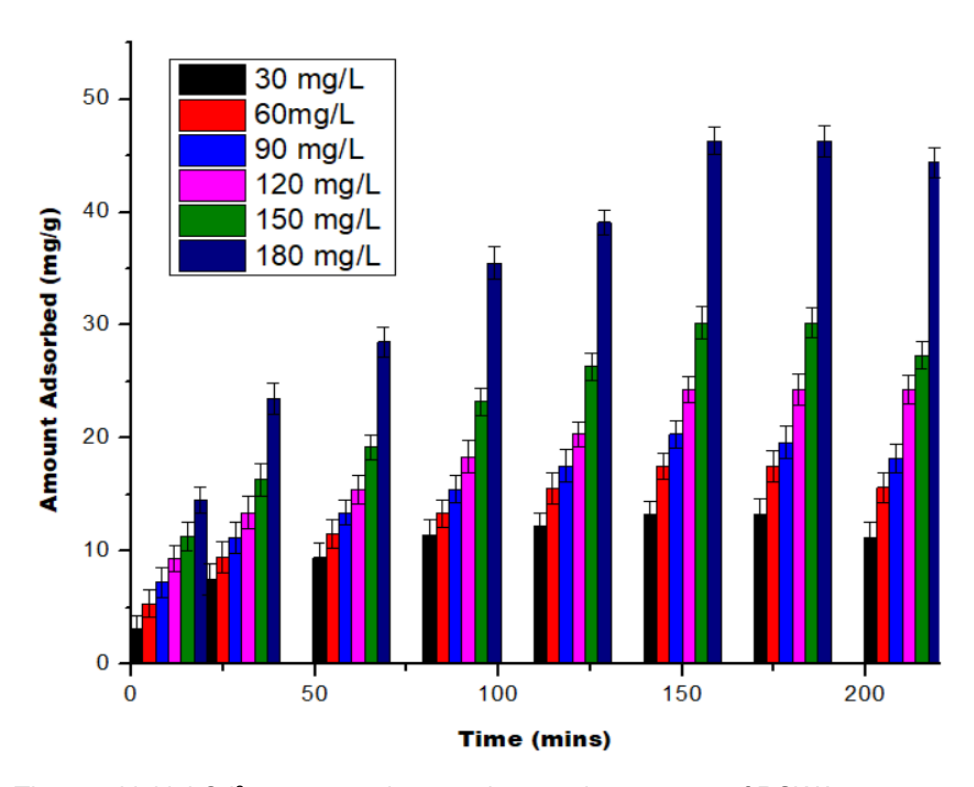


Fig. 4. Time and initial Cd2+ concentrations on the sorption potency of RSWA

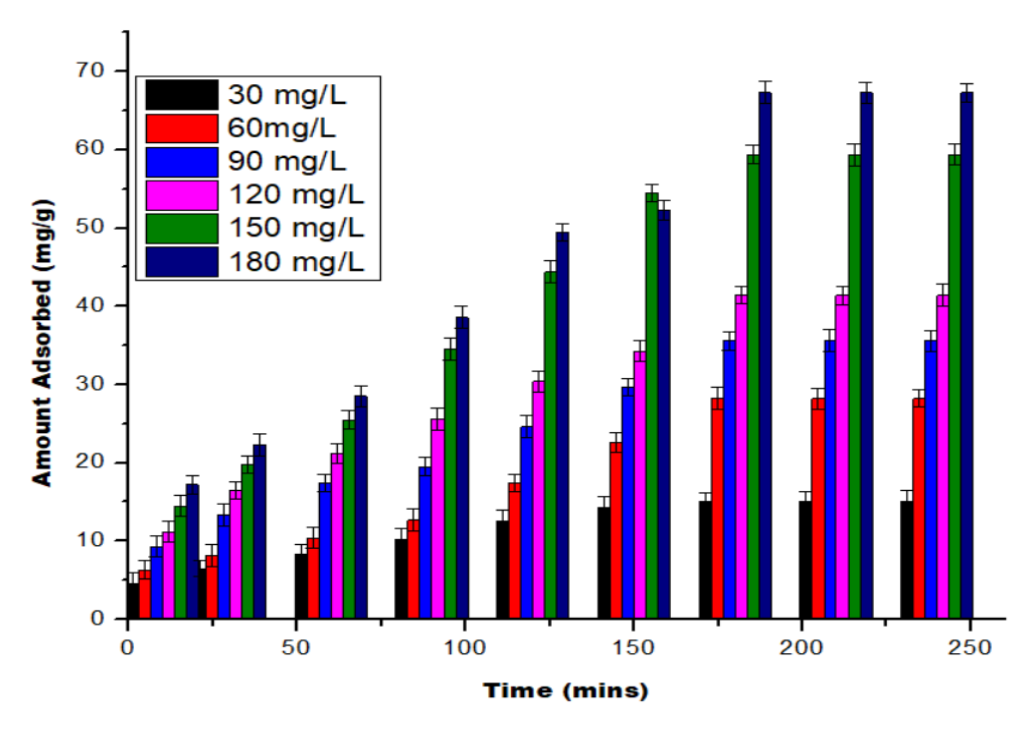


Fig. 5. Time and initial Cd2+ concentrations on the sorption potency of SWBA

Effect of pH on the adsorption of Cd^{2+} ions

For RSWA, adsorption increased from 52.5% at pH 2 to a maximum of 78.6% at pH 5, whereas for SWBA, adsorption increased from 59.8% at pH 2 to 84.1% at pH 6, as depicted in Fig. 6. This suggests that at lower pH levels, competition between H⁺ ions and the pollutants for adsorption sites was strong, reducing the efficiency of pollutant uptake (Akinhanmi et al. 2020; Ofudje et al. 2020a). As pH increased, the availability of functional groups (-COO-, C=C, C=O and C-O) on the adsorbent surface increased, thereby enhancing pollutant binding. The pH_{PZC} of SWBA (4.51) was slightly higher than that of RSWA (4.25), indicating a slight shift in surface charge behavior due to biochar activation. Since the point of zero charge (pH_{PZC}) represents the pH at which the adsorbent's surface has a neutral charge, this difference suggests that SWBA might exhibit a stronger adsorption affinity for cationic pollutants at pH levels above 4.51, whereas RSWA may be more effective at slightly lower pH conditions. At pH 8, Cd²⁺ ion adsorption decreased to 46.8%. This decline may be due to electrostatic repulsion, reducing binding efficiency for RSWA and in the case of Cd²⁺ ions, at high pH, may start precipitating as Cd(OH)2 rather than adsorbing onto the surface, lowering the observed adsorption capacity (Bharathi and Ramesh 2013; Akinhanmi et al. 2020).

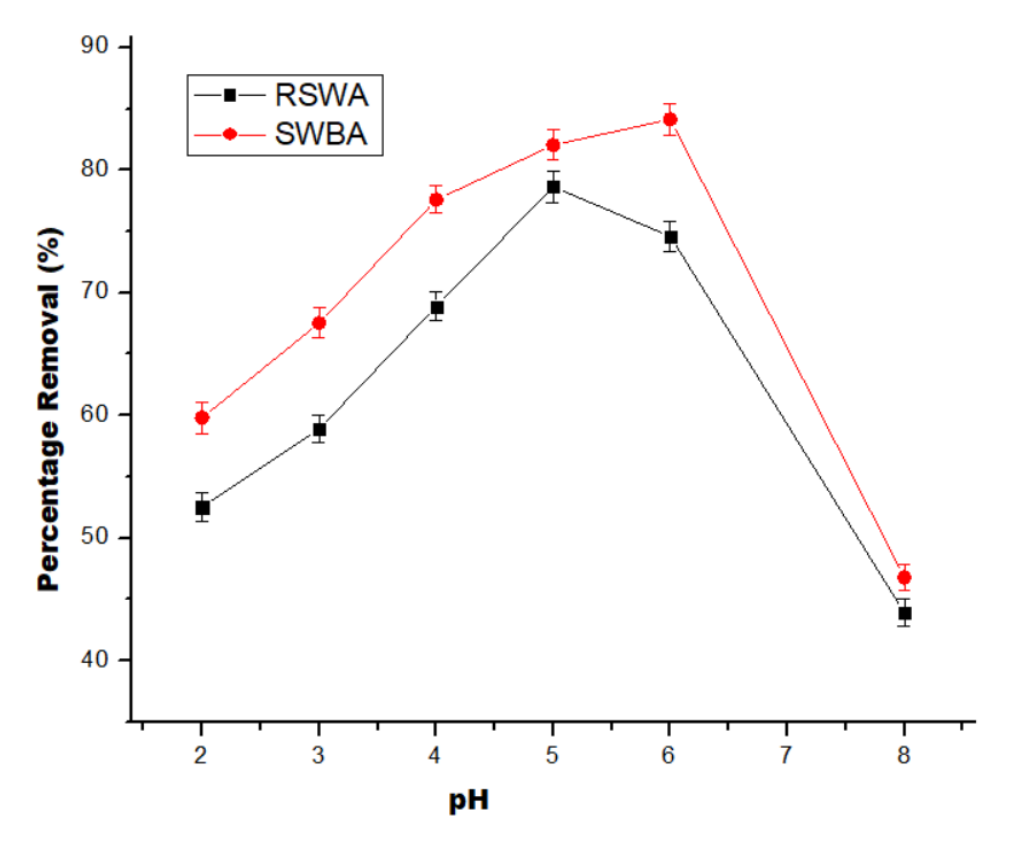


Fig. 6. Influence of pH on the adsorption capacity of Cd²⁺ by RSWA and SWBA

The adsorbent (valorized wood meal) contained various functional groups such as -OH, -COOH, and -NH₂, which can gain or lose protons (H⁺) depending on the pH of the solution. At low pH (acidic conditions, pH 2 to 3), more H⁺ ions were present in the solution, leading to protonation (gain of H⁺), making the adsorbent surface positively charged. However, at high pH (pH 6 to 8), the presence of fewer H⁺ ions resulted in deprotonation (loss of H⁺), giving rise to a negatively charged surface (EL-Shimaa et al. 2021; Ofudje et al. 2023). At Low pH (pH 2 to 3), the adsorbent surface being positively charged, and since Cd²⁺ ions are also positively charged, electrostatic repulsion occurred, limiting adsorption which further explains the relatively lower Cd²⁺ adsorption at pH 2 (59.8 mg/g) and pH 3 (67.5 mg/g) (EL-Shimaa et al. 2021; Uzosike et al. 2022; Ofudje et al. 2023). However, at optimal pH (pH 5 and 6), the adsorbent undergoes partial deprotonation, elevating the density of the negative charge, and this enhances electrostatic attraction and ion exchange between Cd2+ and negatively charged surface sites, leading to higher value (84.1% at pH 6). But at high pH (pH 8), the surface remained deprotonated, which should still favor Cd²⁺ adsorption; however, at pH above 6.5, Cd2+ ions start to precipitate as Cd(OH)2, reducing the amount available for adsorption, this results in a significant drop in Cd²⁺ adsorption at pH 8 (46.8%).

Influence of RSWA and SWBA Dosages

The effect of the dosage amounts of the biochar samples on the adsorption capacity of Cd²⁺ is depicted in Fig. 7. It was deduced that for RSWA, adsorption increased from 51.7% (at 10 mg dosage) to a peak of 77.3% (at 30 mg dosage), while for

SWBA, adsorption increased from 59.0% (at 10 mg dosage) to a peak of 85.1% (at 25 mg dosage), as shown in Fig. 7. The increase occurred because of more active sites for adsorption, improving pollutant removal efficiency, and beyond this point, further increasing the adsorbent dosage did not improve adsorption significantly, suggesting that most available adsorption sites were already occupied (Bharathi and Ramesh 2013). At higher dosages (35 to 40 mg/L), adsorption capacity declined to 69.1% at 35 mg and 60.1% at 40 mg for RSWA, while that of SWBA dropped to 81.1% at 35 mg and 73.9% at 40 mg. This decline is likely due to adsorbent agglomeration caused by excess adsorbent particles which may clump together, reducing the available surface area for adsorption (Bharathi and Ramesh, 2013). Also, with excessive adsorbent, the amount of pollutant per unit adsorbent decreased, leading to lower adsorption efficiency per gram of adsorbent (Akinhanmi *et al.* 2020; Ofudje *et al.* 2023).

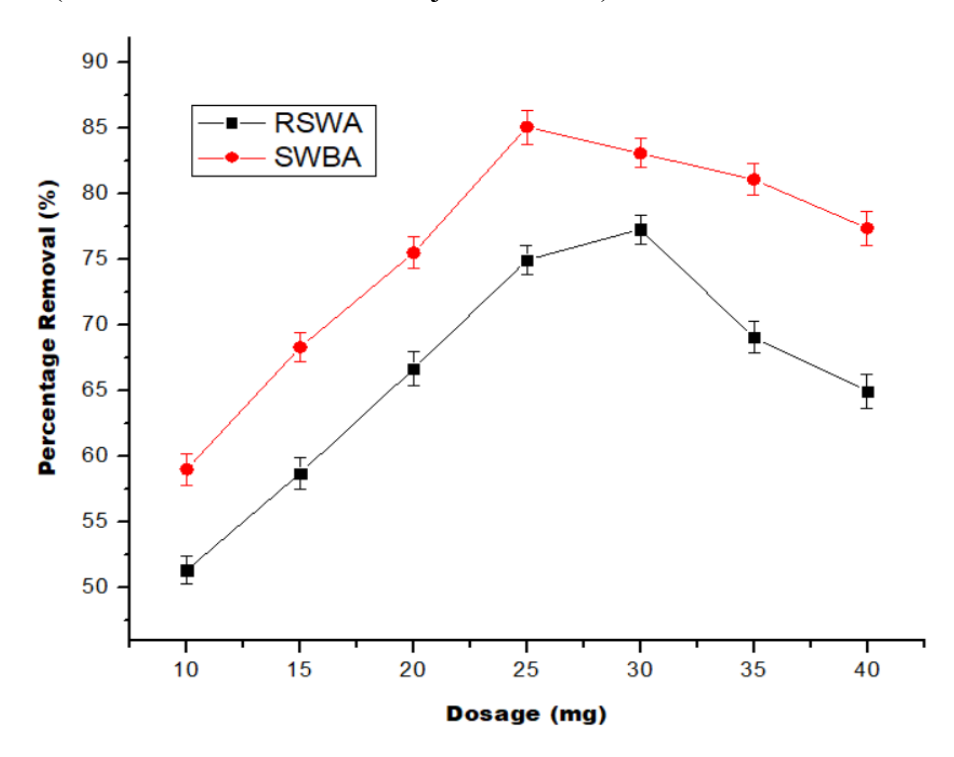


Fig. 7. Influence of RSWA and SWBA dosages on the sorption of Cd2+ ions

Kinetics Studies

Pseudo-first-order kinetics

This model can be expressed as (Lagergren, 1898; Bharathi and Ramesh, 2013; Chauhan, et al. 2023),

$$\log(Q_e - Q_t) = \log Q_e - \frac{k_1}{2.303}t \tag{4}$$

where Q_t denotes adsorption amount at time t (mg/g), k_1 is the pseudo-first-order rate constant (min⁻¹), and t is time (min). Plots of $\log(Q_e - Q_t)$ against t, as shown in Fig. 8, were used to estimate the parameters listed in Tables 2 and 3. For both RSWA and SWBA, the experimental adsorption capacity $Q_e(\exp)$ rose with an increase in initial concentration, meaning that higher pollutant concentrations led to greater adsorption onto sawmill adsorbent. However, the calculated adsorption capacities ($Q_e(\operatorname{cal})$) showed

deviations from $Q_{e(exp)}$, suggesting that the first-order model did not accurately predict adsorption. The coefficients of determination (R²) for Cd²⁺ ranged from 0.897 to 0.954, while for RSWA they ranged from 0.975 to 0.994, indicating a good fit for describing the adsorption process especially in the case of RSWA.

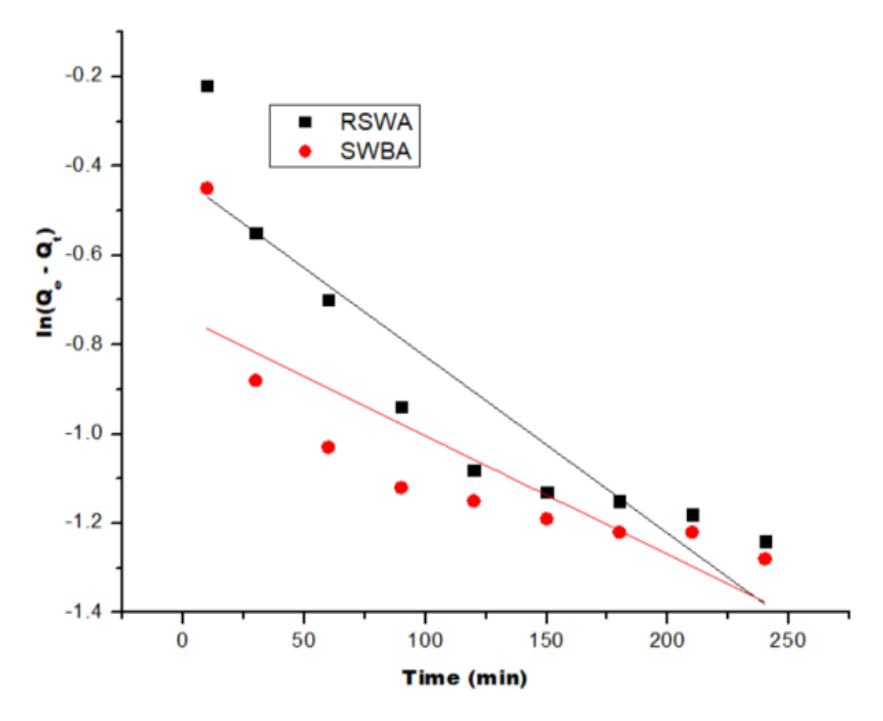


Fig. 8. Plots of pseudo-first-order kinetics for the adsorption of Cd2+ by RSWA and SWBA

Pseudo-second-order kinetics

This model can be expressed as (Ho and McKay 1999; Bharathi and Ramesh, 2013; Chauhan *et al.* 2023),

$$t/Q_t = \frac{1}{k_2}Q_t + t/Q_e \tag{5}$$

where Q_t and Q_e are as previously defined, and k_2 stands for the pseudo-second-order rate constant (g/mg·min). Plots of t/Q_t against t, as shown in Fig. 9, were used to estimate the parameters listed in Tables 2 and 3. The $Q_e(cal)$ values for both adsorbents were much closer to the $Q_e(exp)$ values compared to the first-order model, indicating that adsorption followed this model (Ho and McKay 1999). The validation of best fit was achieved using root mean square errors (RMSE).

$$RMSE = \sqrt{\frac{\sum_{i}^{N} (Q_{(exp)} - Q_{(cal)})^{2}}{N}}$$
(6)

In Eq. 6, N denotes the number of data points, and other parameters are as previously defined. The R² values for SWBA adsorption ranged from 0.992 to 0.998, while for RSWA it ranged from 0.988 to 0.997, confirming a much better fit and this was supported from the lower values obtained for %SSE.

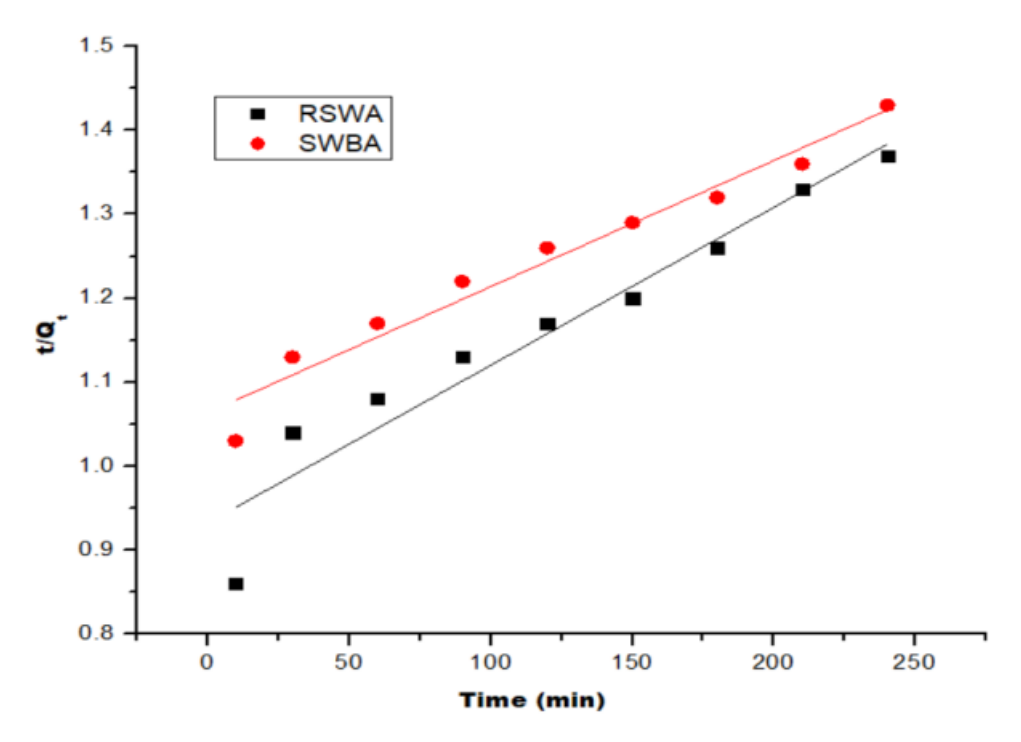


Fig. 9. Plots of pseudo-second-order kinetics for the adsorption of Cd2+ by RSWA and SWBA

Intraparticle Diffusion Model

The intraparticle diffusion model is commonly used to describe the adsorption process when diffusion within the pores of the adsorbent plays a significant role in controlling the rate of adsorption.

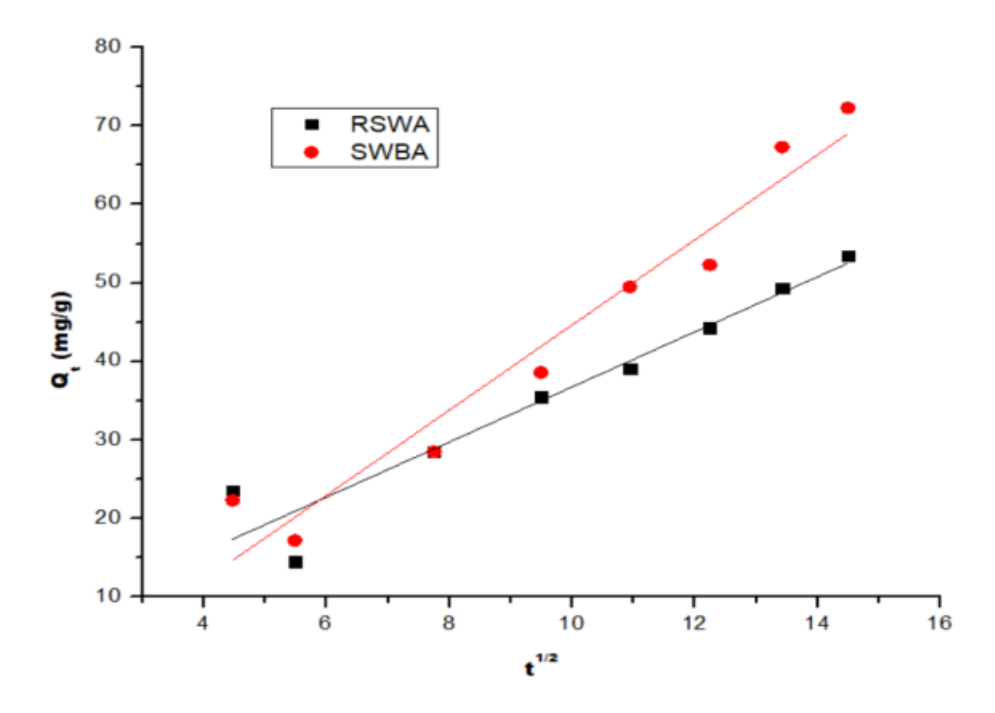


Fig. 10. Plots of intraparticle diffusion kinetics for the adsorption of Cd2+ by RSWA and SWBA

This model helps determine whether the sorption process is explained by intraparticle diffusion, film diffusion, or both. The model can be represented as (Bharathi and Ramesh 2013; Oyelude *et al.* 2018; Chen *et al.* 2019),

$$Q_t = k_p t^{1/2} + C_i \tag{7}$$

where k_p stands for the intra-particle diffusion rate constant (mg/g/min^{1/2}), and C_i represents boundary layer thickness. The plots of t/Q_t against $t^{1/2}$ as shown in Fig.10 were used to estimate the parameters listed in Tables 2 and 3.

Table 2. Kinetics Studies of RSWA as Adsorbent for the Uptake of Cd²⁺

	C _o (mg/L)	30 mg/L	60 mg/L	90 mg/L	120 mg/L	150 mg/L	180 mg/L
der	$Q_{\rm e(exp)}$ (mg/g)	15.101	28.200	35.600	41.400	59.400	67.300
	$Q_{\rm e(cal)}$ (mg/g)	10.561	23.120	39.031	47.811	53.005	62.769
First order	<i>k</i> ₁ (mins⁻¹)	0.026	0.035	0.053	0.065	0.077	0.082
Fi	R^2	0.897	0.915	0.946	0.925	0.941	0.954
	% SSE	0.134	0.142	0.047	0.063	0.032	0.117
	Q _{e(cal)} (mg/g)	13.074	29.873	36.017	41.573	59.471	69.543
Second	k₂ (g/mg/min)	0.041	0.062	0.073	0.088	0.104	0.121
Sec	R ²	0.996	0.998	0.995	0.994	0.992	0.998
	% SSE	0.015	0.016	0.015	0.002	0.002	0.014
£	α(mg/g/mins)	1.215	1.813	2.281	2.619	3.401	5.217
Elovich	$oldsymbol{eta}(\mathrm{g}/\mathrm{mg})$	0.132	0.162	0.032	0.836	0.237	0.185
ᇳ	R^2	0.985	0.966	0.945	0.996	0.976	0.986
Intra particle diffusion	Κ _p (mg/g/mins ^{1/2})	1.113	3.707	6.172	7.301	9.074	12.007
	C _i (mg/g)	-0.228	-0.052	1.142	1.133	2.051	2.984
	R^2	0.994	0.989	0.979	0.986	0.995	0.994

Table 3. Kinetics Studies of SWBA as Adsorbent for the Uptake of Cd2+

	C _o (mg/L)	30 mg/L	60mg/L	90 mg/L	120 mg/L	150 mg/L	180 mg/L
	Q _e (exp) (mg/g)	13.200	17.500	20.330	24.300	30.200	46.300
+ <u>-</u>	Q _e (cal) (mg/g)	9.303	12.326	17.024	21.245	36.205	41.321
First	<i>k</i> ₁ (mins ⁻¹)	0.013	0.018	0.024	0.045	0.621	0.810
ш ō	R^2	0.975	0.994	0.981	0.990	0.980	0.978
	% SSE	0.113	0.115	0.013	0.018	0.022	0.013
_	Q _e (cal)	12.393	18.202	21.053	23.304	29.006	45.509
2nd order	k ₂ (g/mg/min)	0.431	0.464	0.633	0.833	1.062	1.521
210	R^2	0.996	0.989	0.997	0.989	0.988	0.995
	% SSE	0.012	0.006	0.011	0.005	0.011	0.008
Elovich	α (mg/g/mins)	0.460	0.654	0.840	1.007	1.129	1.324
	β (g/mg)	0.016	0.065	0.081	0.107	0.253	0.409
	R^2	0.946	0.934	0.985	0.989	0.967	0.984
	K _p mg/g/mins ^{1/2})	1.006	1.242	2.809	3.722	5.143	6.318
Intra particle diffusion	C (mg/g)	0.212	0.458	1.049	2.023	4.371	5.272
	R²	0.992	0.989	0.984	0.984	0.984	0.936

It was observed that the k_p values, which indicate the rate of diffusion inside the pores of the adsorbent, increased with increasing initial pollutant concentration, meaning that diffusion plays a significant role at higher concentrations. The C values suggest that external surface adsorption is also involved, especially at lower concentrations, while the R^2 values were consistently high (above 0.98 for Cd^{2+} and MG), indicating that diffusion is an important step in the adsorption mechanism.

The kinetic data for Cd²⁺ adsorption by SWBA and RSWA fit well with both the pseudo-first-order and pseudo-second-order models, and the intraparticle diffusion model also showed good agreement. This combination of findings suggests that the overall rate of the adsorption process was diffusion-limited, occurring primarily within a network of small pores (Hubbe *et al.* 2019).

Analysis of Isotherms

Langmuir isotherm analysis

The Langmuir isotherm can be represented thus (Bharathi and Ramesh 2013; Shanmugarajah *et al.* 2018),

$$\frac{C_e}{Q_e} = \frac{1}{bq_m} + \frac{C_e}{Q_m} \tag{8}$$

with the maximum adsorption capacity given as $Q_{\rm max}$ (mg/g), b (L/mg) denotes the constant of Langmuir, and the equilibrium concentration given as $C_{\rm e}$ (mg/L), and $Q_{\rm e}$ (mg/g) is as previously defined. The graphical representation of this model is shown in Fig. 11, and the values obtained are as presented in Table 4.

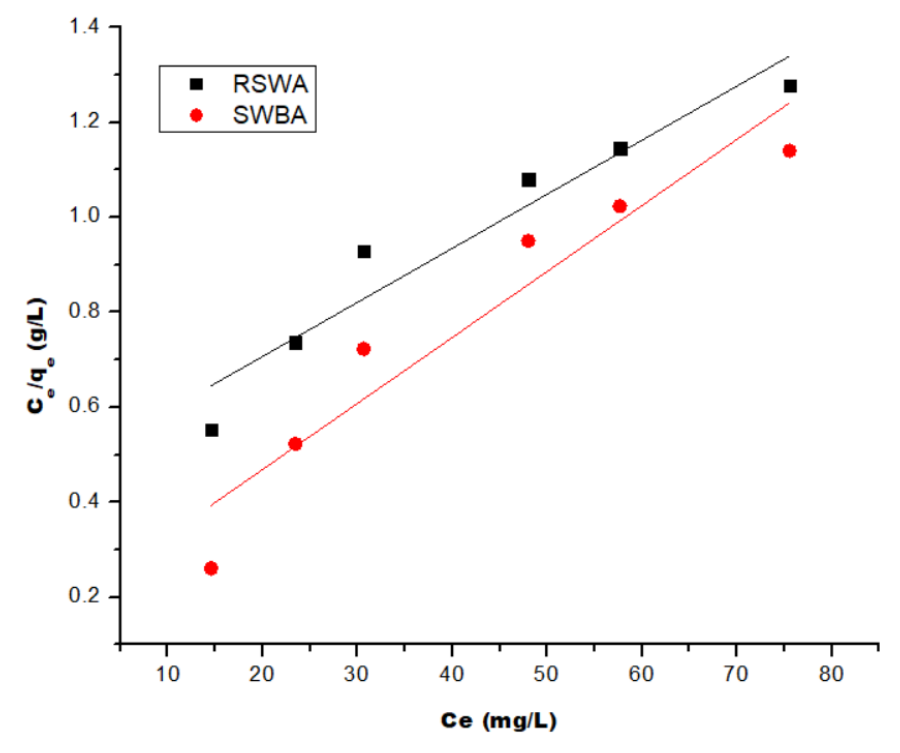


Fig. 11. Langmuir isotherm for the adsorption Cd2+

The higher $Q_{\rm max}$ for SWBA (52.236 mg/g) compared to RSWA (41.242 mg/g) suggests that the valorized sawmill waste had more available adsorption sites for Cd²⁺. The expression for the separation factor ($R_{\rm L}$) which can be used to predict the favorability of adsorption is given as:

$$R_L = \frac{1}{(1+bC_o)} \tag{9}$$

The lower R_L value for SWBA (0.058) compared to RSWA (0.107) confirms that Cd^{2+} adsorption was more favorable. Higher b value for SWBA (0.836) suggests stronger adsorption energy, making Cd^{2+} more tightly bound to the SWBA and the R^2 values suggests that the adsorption of Cd^{2+} by SWBA followed the Langmuir model more closely than RSWA.

Freundlich isotherm analysis

The Freundlich model is more applicable when the adsorption sites have different energy levels. It can be expressed as (Bharathi and Ramesh 2013; Ofudje *et al.* 2023):

$$InQ_e = InK_F + \frac{1}{n}C_e \tag{10}$$

The Freundlich constant is given as K_F (mg/g) which defines adsorption capacity, and 1/n is the adsorption intensity parameter, when 0 < 1/n < 1, the adsorption being favorable. The graphical representation of this model is shown in Fig. 12, from where the values listed in Table 4 were obtained. The higher K_F for SWBA (41.1 mg/g) suggests that the adsorption was more efficient compared to RSWA (34.2 mg/g). The lower 1/n for SWBA (0.013) suggests stronger interactions and less tendency for desorption. Judging from R^2 values, the adsorption of Cd^{2+} by both adsorbents fit Freundlich isotherms.

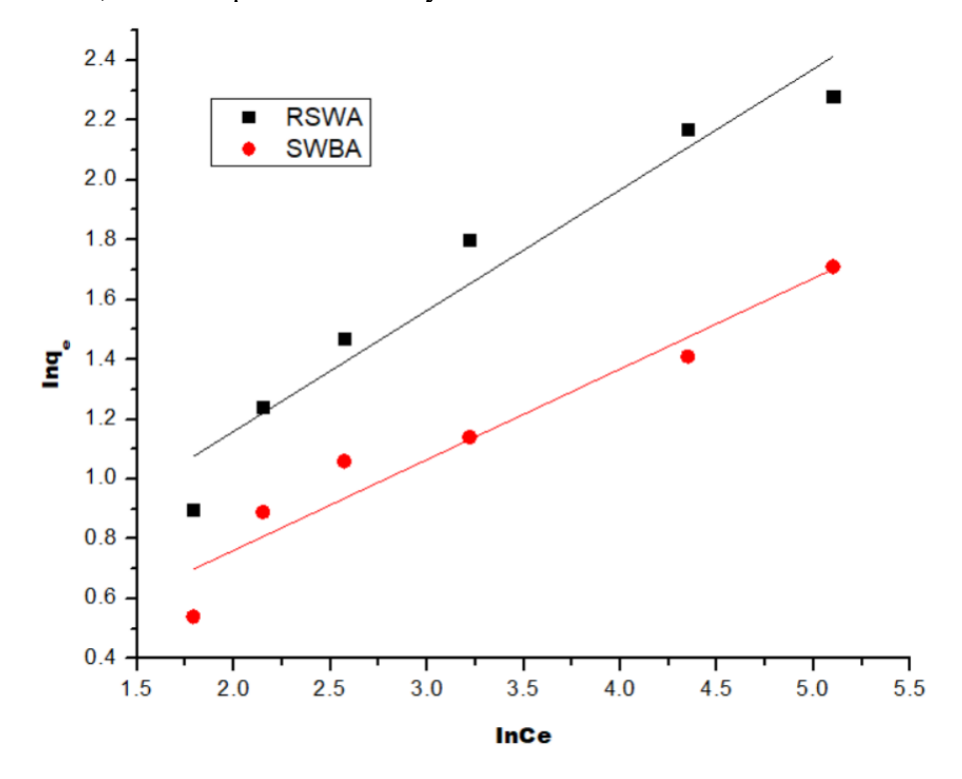


Fig. 12. Freundlich isotherms for the adsorption of Cd2+

Dubinin–Radushkevich (D-R) isotherm analysis

The D-R isotherm explains the porosity and energy of adsorption, distinguishing between physisorption and chemisorption. The model, the Polanyi potential, and mean adsorption energy can be expressed as (Duan *et al.* 2020; Uzosike *et al.* 2022):

$$InQ_e = InQ_m - InK_{DR}^{\varepsilon^2}$$
(11)

$$\varepsilon = RTIn(1 + \frac{1}{C_e}) \tag{12}$$

$$E = 1/\sqrt{2K_{DR}} \tag{13}$$

The amount of pollutant adsorbed per unit weight of the adsorbent at equilibrium (Q_e) is expressed in mol/g, while Q_m represents the maximum adsorption capacity for monolayer coverage (mol/g). The mean sorption energy, associated with the activity coefficient (K_{DR}) , is measured in mol²/kJ². The Polanyi potential constant is denoted as ϵ , R (8.3145 J·mol⁻¹) is the ideal gas constant, and T represents the absolute temperature in Kelvin.

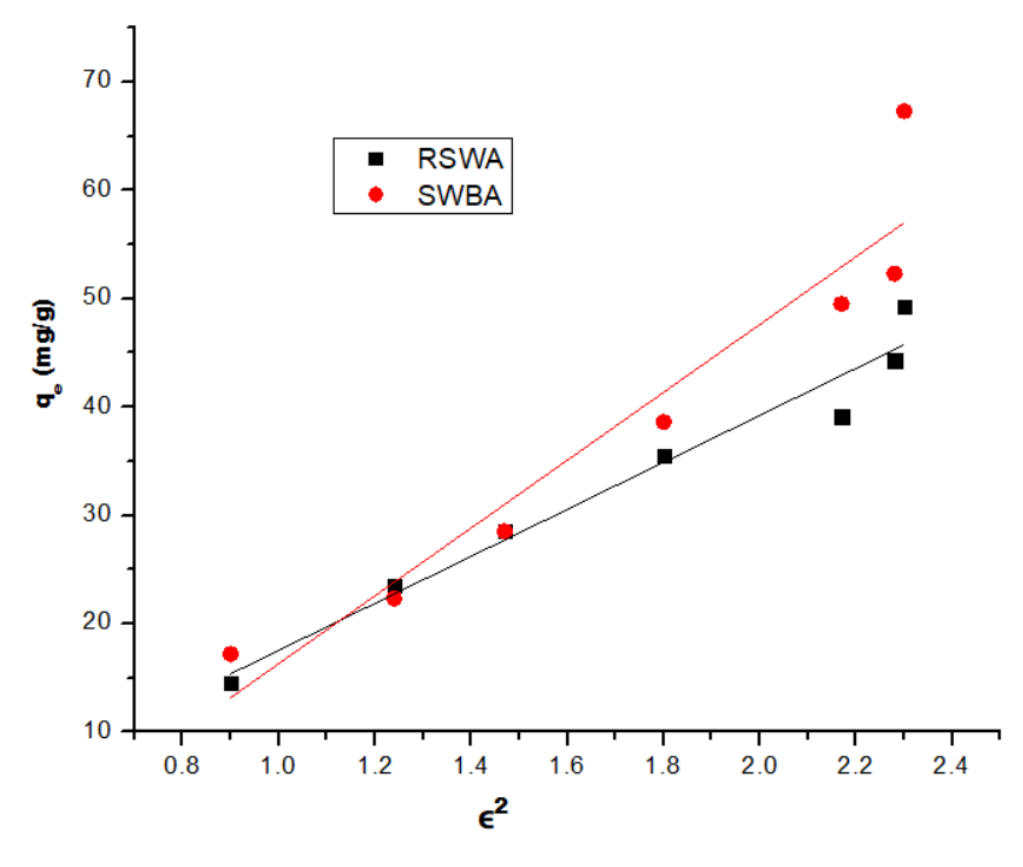


Fig. 13. Dubinin-Radushkevich isotherm plots

The model is represented graphically in Fig. 13, while the obtained values are provided in Table 4. The higher Q for SWBA (45.0 mg/g) than RSWA (37.5 mg/g) further confirms higher adsorption efficiency for the raw sample, while higher ε for thermally treated sample (0.631) suggests that the raw sample adsorption is more energy-dependent, possibly due to stronger ion-dipole interactions with functional groups on the

sawmill waste. The low E values (both < 8 kJ/mol) indicate physisorption dominates, meaning that the adsorption is mostly due to weak Van der Waals forces rather than strong chemical bonding. Since R^2 values for both adsorbents (RSWA = 0.988) and (SWBA = 0.978) is high enough, it confirms a good fit to the D-R model.

Table 4. Isotherms Constants of Sawmill Waste Valorization as Adsorbent for Cadmium Ions Adsorption

	Parameters	RSWA	SWBA
Langmuir	Q _{max} (mg/g)	41.242	52.236
	R∟	0.107	0.058
	b (mg/L)	0.642	0.836
	R ²	0.867	0.927
Freundlich	$K_{\rm F}$ (mg/g)(mg/L) ^{-1/2}		
		34.236	41.132
	1/n	0.374	0.013
	R ²	0.934	0.998
Dubinin-Radushkevich	Q (mg/g)	37.481	45.023
	ε (molJ ⁻¹) ²	0.442	0.631
	E (kJmol ⁻¹)	0.966	0.537
	R ²	0.988	0.978

Table 5 provides a literature review comparing the performance of various adsorbent materials in the removal of malachite green and Cd²⁺ions from aqueous solutions.

Table 5. Various Adsorbents and their Adsorption Capacities towards Cd²⁺ lons

Adsorbents	Q _{max} (mg/g)	References	
Orange peel	27.9	Akinhami <i>et al</i> . 2020	
Modified cassava tuber bark waste (MCTBW)	33.4	Ofudje <i>et al.</i> [9]	
Raw cassava tuber bark waste (RCTBW)	73.2	Ofudje <i>et al.</i> 2020a	
Sawdust	47.9	Okpara <i>et al</i> . 2023	
Tagaran natural clay	18.8	Bakhtyar <i>et al.</i> 2019	
Poplar sawdust biochar	49.3	Cheng <i>et al</i> . 2021	
Activated Carbon from Bombax Ceiba Fruit Shell	4.4	Rumpa <i>et al</i> . 2020	
Barley biochar	33.6	Simon et al. 2024	
Sawdust biochar	25.8	Simon <i>et al.</i> 2024	
Natural Montmorillonite-Based Magsorbent	36.60	Sibel <i>et al</i> . 2020	
RSWA	78.6	This study	
SWBA	85.4	This study	

The studied adsorbent demonstrated great adsorption capacity, reaching 85.4 mg/g for SWBA and 78.6 mg/g for RSWA, surpassing many alternative materials. This comparison highlights the valorized sawmill wood waste's potential as an effective, cost-efficient, eco-friendly, and sustainable solution for treating malachite green and Cd²⁺ions pollutants in wastewater.

Effect of Temperature and Thermodynamic Evaluations

The adsorption capacity for both adsorbents increased as temperature rose from 25 to 40 °C for RSWA and 45 °C for SWBA, as shown in Fig. 14. This implies that the adsorption process is endothermic, meaning higher temperatures enhance the interaction between the adsorbate and the adsorbent (Uzosike *et al.* 2022; Ofudje *et al.* 2023). It was observed that RSWA reached its maximum adsorption at 40 °C (78.46 %), while SWBA peaked slightly later at 45 °C (85.4%). This indicates that at moderate temperatures, the adsorbent surface was more active, leading to greater pollutant uptake. However, after 45 °C, the adsorption started to decline for both adsorbents, and at 55 °C, RSWA adsorption dropped to 67.4%, while SWBA adsorption decreased significantly to 61.4%. The decline suggests that desorption or weakening of interactions occurs at higher temperatures, increased solubility of Cd²⁺, leading to decreased retention, and or possible structural changes in the adsorbent, reducing its ability to bind pollutants (Guruprasad *et al.* 2024).

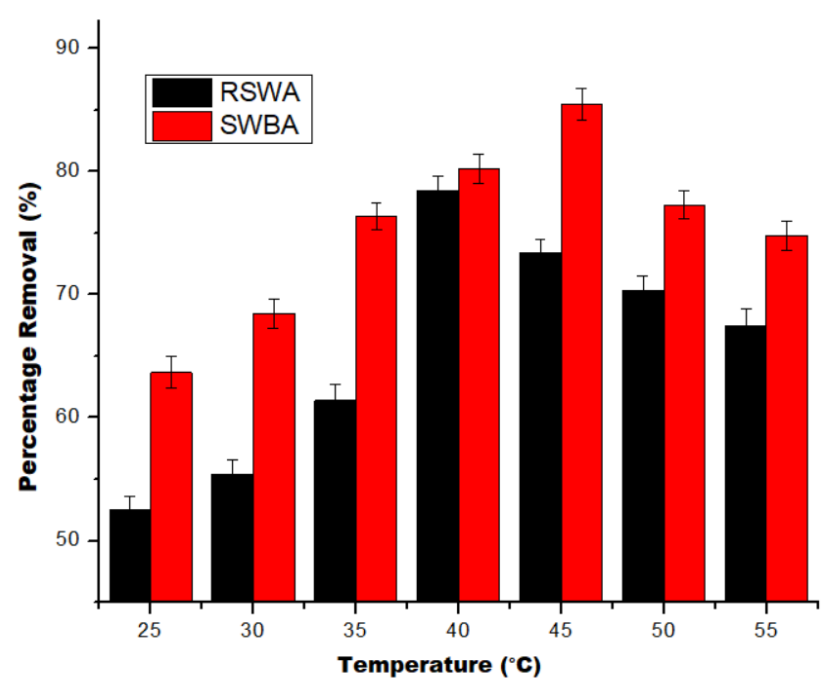


Fig. 14. Plot of temperature effects on the adsorption capacity

Thermodynamic studies provide insights into the feasibility, spontaneity, and energy changes associated with adsorption and the key thermodynamic parameters analyzed are Gibbs free energy change (ΔG , kJ/mol), enthalpy change (ΔH , kJ/mol), and entropy change (ΔS , J/mol·K) were investigated using the following Eqs. 14 to 16 (Sarada *et al.* 2017; Ofudje *et al.* 2023):

$$K_d = \frac{q_e}{C_e}$$
 (14)

$$\ln K_d = \frac{\Delta S^o}{R} - \frac{\Delta H^o}{RT} \tag{15}$$

$$\Delta G^o = RTInK_d \tag{16}$$

The plots of InK_L against 1/T, as shown in Fig. 15, were used to deduce the values presented in Table 6.

The results reveal that the Gibbs free energy change ΔG values for both adsorbents are negative at all temperatures, confirming that adsorption was spontaneous (Adeogun *et al.* 2018; Ofudje *et al.* 2023).

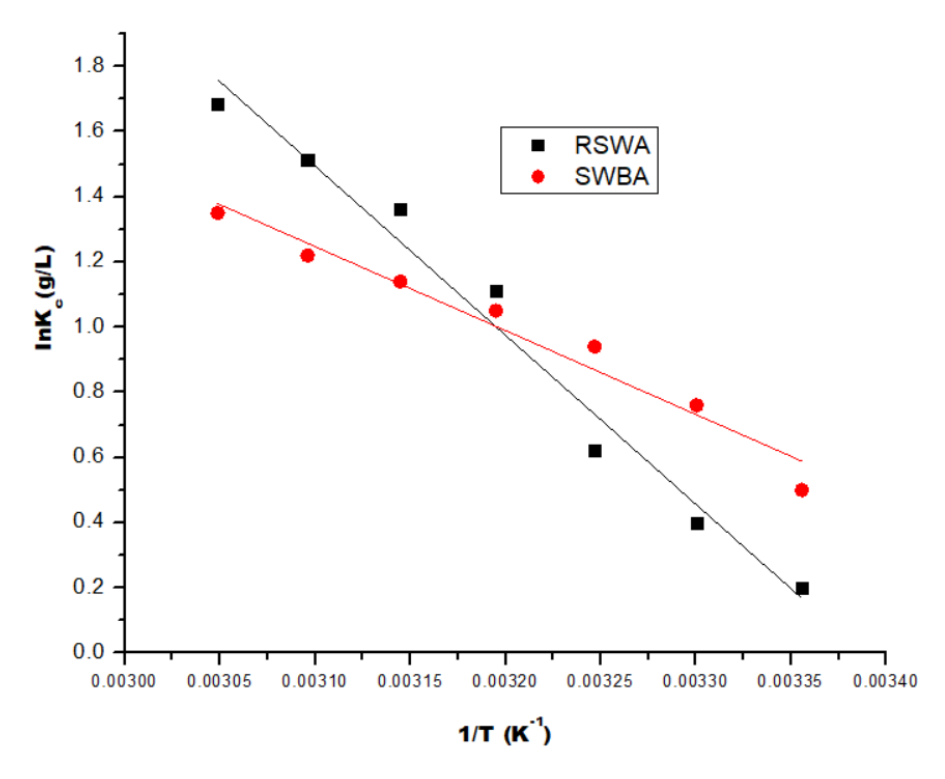


Fig. 15. Thermodynamic plots for the adsorption of Cd2+

Table 6. Thermodynamics Parameters of Sawmill Waste Valorization as Adsorbent for Cd²⁺ Adsorption

		RSWA		SWBA		
<i>T</i> (K)	ΔG (kJ/mol)	ΔΗ (kJ/mol)	ΔS (J/mol·K)	ΔG (kJ/mol)	Δ <i>H</i> (kJ/mol)	ΔS (J/mol·K)
298	-1.02			-0.68		
303	-1.31			-1.07		
308	-1.62			-1.46		
313	-2.36	22.35	14.04	-1.86	14.56	7.05
318	-2.57			-2.45		
323	-3.28			-2.157		
328	-6.85			-3.74		

It was noticed that as temperature increased (from 298 to 328 K), ΔG became more negative, indicating that higher temperatures favored adsorption, making it more thermodynamically feasible (Akinhanmi *et al.* 2020; Ofudje *et al.* 2023). For RSWA, ΔG changed from -1.02 kJ/mol (298 K) to -6.85 kJ/mol (328 K), while for SWBA, it changed from -0.68 kJ/mol (298 K) to -3.74 kJ/mol (328 K). In the case of enthalpy change (ΔH), the values obtained for RSWA and SWBA were 22.35 and 14.56 kJ/mol, respectively, suggesting endothermic adsorption (Adeogun *et al.* 2018; Akinhanmi *et al.* 2020). Endothermic behavior suggests that heat is absorbed during adsorption, and the higher ΔH for RSWA (22.35 kJ/mol) than for SWBA (14.56 kJ/mol) implies that RSWA adsorption requires more energy, possibly due to weaker initial interactions that need heat to improve adsorption. For entropy change (ΔS), the positive ΔS values (14.04 J/mol·K for RSWA and 7.05 J/mol·K for SWBA) indicate that adsorption increases randomness at the adsorbent-solution interface (Uzosike *et al.* 2022).

Desorption Study

The desorption graph illustrates the percentage desorption (PD%) of Cd²⁺ ions from the surface of the adsorbent over multiple regeneration cycles using valorized wood residues from a sawmill, as shown in Fig. 16.

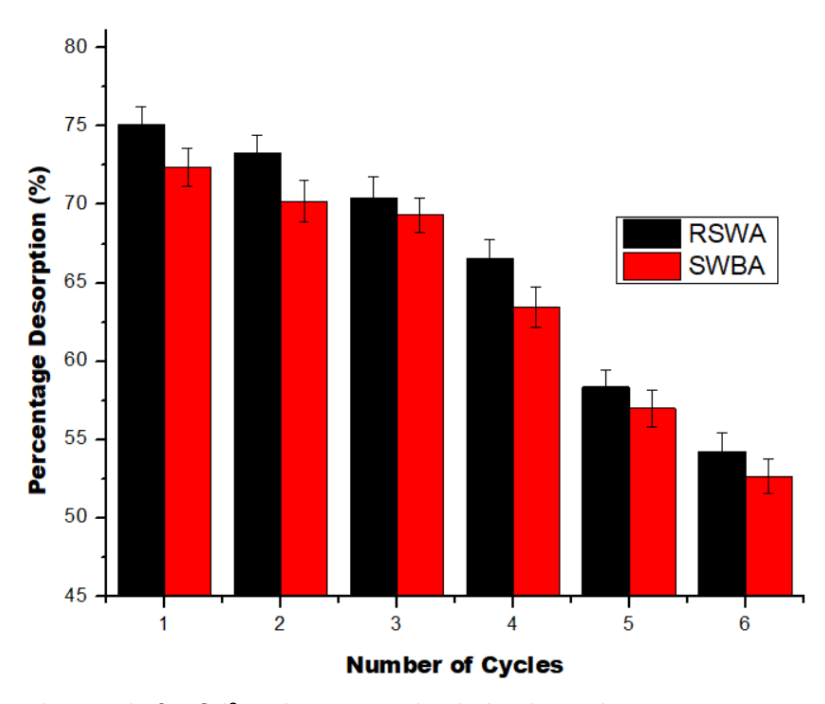


Fig. 16. Desorption study for Cd²⁺ using raw and valorized wood waste

Among the regeneration agents used, HCl was found to be the most effective, yielding the highest desorption efficiency across repeated cycles and was therefore selected for subsequent experiments. It was observed that both RWSA and SWBA exhibited a gradual decrease in desorption efficiency as the number of regeneration cycles increased. The desorption percentage started relatively high (75% for RWSA and 72% for SWBA in Cycle 1), but it declined steadily with each cycle, reaching around 50% or lower by Cycle 6. Throughout all cycles, RWSA maintained a slightly higher desorption percentage than SWBA. The data suggests that valorized wood waste sawmill

material is reusable for Cd²⁺ions adsorption but with a declining efficiency after multiple cycles.

While this does suggest a limited number of effective regeneration cycles, the adsorbent still retained a substantial proportion of its capacity after several cycles, which supports short- to medium-term reusability. On a large scale, this trend could increase operational costs due to the need for periodic replenishment or reactivation of the adsorbent. However, considering the low-cost and abundant nature of the raw material (sawmill waste), this drawback may be economically manageable compared to synthetic adsorbents.

Adsorption Mechanism

The adsorption mechanism may be controlled by electrostatics, ion exchange, and complexation with functional groups on the adsorbent's surface (Gupta and Suhas 2009; Akinhanmi *et al.* 2020). Based on kinetics evaluation, the adsorption mechanism of Cd^{2+} onto SWBA and RSWA involves a diffusion-limited process, in which the metal ions diffused into a microporous matrix and adsorption occurs at internal active sites. This is confirmed by the strong fit of the intraparticle diffusion model, with the kinetics governed by a combination of pseudo-first- and pseudo-second-order models. Also, from thermodynamic investigation, the ΔH values further help elucidate the adsorption mechanism. According to typical adsorption energy ranges, enthalpy changes between 2 and 40 kJ/mol suggest physical adsorption via hydrogen bonding and dipole interactions; values around 40 kJ/mol point to coordination exchange, while those exceeding 60 kJ/mol indicate chemical bonding (Zhao *et al.*, 2014). In this study, the enthalpy values for RSWA (22.4 kJ/mol) and SWBA (14.6 kJ/mol) fall within the range for physisorption, confirming that physical interactions dominate the adsorption mechanism.

The pH also plays a critical role in this process; at higher pH values, increased ionization of the wood's surface functional groups enhances Cd²⁺ adsorption capacity. Sawmill wood adsorbents can effectively adsorb cadmium ions through electrostatic interactions between the metal positive charged surface and lignocellulosic functional groups in the wood which are negatively charged (Gupta and Suhas 2009).

CONCLUSIONS

From the results obtained, the following deduction were made:

- 1. Sawmill wood waste was utilized as a sustainable material for removing Cd²⁺ ions from wastewater.
- 2. The biochar adsorbent (SWBA) gave superior adsorption capacity in comparison to raw sawmill waste adsorbent (RSWA), influencing both adsorption capacity and kinetics.
- 3. Equilibrium time was reached faster for RSWA (150 min) than for SWBA (180 min), while the sorption process was found to be pH-dependent, with optimal removal attained at pH of 5 to 6.
- 4. Scanning electron microscopy (SEM) analysis confirmed a rough, porous structure that aids contaminant binding but undergoes morphological changes post-adsorption.

5. Thus, sawmill wood residue and its biochar product can be regarded as viable adsorbents for wastewater treatment, supporting heavy metal removal and sustainability.

ACKNOWLEDGMENTS

The authors extend appreciation to the Northern Border University, Saudi Arabia, for supporting this work through the project number "NBU-CRP-2025-2985". Furthermore, authors wish to appreciate the financial support *via* Princess Nourah bint Abdulrahman University Researchers Supporting Project number PNURSP2025R65, Princess Nourah bint Abdulrahman University, Riyadh, Saudi Arabia.

REFERENCES CITED

- Abate, G. Y., Alene, A. N., Habte, A. T., and Getahun, D. M. (2020). "Adsorptive removal of malachite green dye from aqueous solution onto activated carbon of Catha edulis stem as a low-cost bio-adsorbent," *Environ. Syst. Res.* 9(9), article 13. DOI: 10. 1186/ s40068- 020- 00191-4
- Adeogun, A. I., Ofudje, E. A., Idowu, M. A., Kareem, S. O., Vahidhabanu, S., and Babu, B. R. (2018). "Biosorption of Cd²⁺ and Zn²⁺ from aqueous solution using tilapia fish scale (*Oreochromis sp*): Kinetics, isothermal and thermodynamic study," *Desal. Water Treat.* 107, 182-194. DOI: 10.5004/dwt.2018.22122.
- Ahmad, A. A., and Hameed, B. H. (2010). "Effect of preparation conditions of activated carbon from bamboo waste for real wastewater," *J. Hazard. Mat.* 173(1-3), 487-493. DOI: 10.1016/j.jhazmat.2009.08.111
- Akinhanmi, T. F., Ofudje, E. A., Adeogun, A. I., Aina, P., and Joseph, I. M. (2020). "Orange peel as low-cost adsorbent in the elimination of Cd(II) ion: Kinetics, isotherm, thermodynamic and optimization evaluations. *Bioresour. Bioprocess.* 7, article 34. DOI: 10.1186/s40643-020-00320-y
- Akrivi, K., Lucyna, L.-A., Kostas, C., Georgios, T., and Angelos, A. (2025). "Wood waste valorization and classification approaches: A systematic review," *Open Research Europe* 5, article 5. DOI.10.12688/openreseurope.18862.1
- Alsawy, T., Rashad, E., El-Qelish, M., and Mohammed, R.H. (2022). "A comprehensive review on the chemical regeneration of biochar adsorbent for sustainable wastewater treatment," *NPJ Clean Water* 29. DOI: 10.1038/s41545-022-00172-3
- Bakhtyar, K. A., Dler, M. S. S. and Stephan. (2019). "Characterization of Tagaran natural clay and its efficiency for removal of cadmium (II) from Sulaymaniyah industrial zone sewage," *Environ. Sc. and Poll. Res.* 27, 38384-38396. DOI: 10.1007/s11356-019-06995-x.
- Balji, G. B., Surya, A., Govindaraj, P., Ponsakthi, and G. M. (2022). "Utilization of fly ash for the effective removal of hazardous dyes from textile effluent," *Inorg. Chem. Commun.* 143, article 109708. DOI: 10.1016/j.inoche.2022.109708
- Bayram, O., Köksal, E., Göde, F., and Pehlivan, E. (2022). "Decolorization of water through removal of methylene blue and malachite green on biodegradable magnetic

- *Bauhinia variagata* fruits," *Int. J. Phytorem.* 24, 311-323. DOI:10.1080/15226514. 2021.1937931
- Bhatnagar, A., and Sillanpaa, M. (2010). "Utilization of agro-industrial and municipal waste materials as potential adsorbents for water treatment—A review," *Chem. Engin. J.* 157(2-3), 277-296. DOI: 10.1016/j.cej.2010.01.007
- Bharathi, K. S., and Ramesh, S. T. (2013). "Removal of dyes using agricultural waste as low-cost adsorbents: A review," *Appl. Water Sci.* 3(4), 773-790. DOI: 10.1007/s13201-013-0117-y
- Chauhan, S., Shafi, T., Dubey, B. K., and Chowdhury, S. (2023). "Biochar-mediated removal of pharmaceutical compounds from aqueous matrices via adsorption," *Waste Dispos. Sustain. Energy* 5, 37-62. DOI: 10.1007/s42768-022-00118-y
- Chen, Y., Shi, J., Du, Q., Zhang, H., and Cui, Y. (2019). "Antibiotic removal by agricultural waste biochars with different forms of iron oxide," *RSC Advances* 9(25), 14143-14153. DOI:10.1039/c9ra01271k
- Cheng, S., Liu, Y., Xing, B., Qin, X., Zhang, C., and Xia, H. (2021). "Lead and cadmium clean removal from wastewater by sustainable biochar derived from poplar saw dust," *J. Clean. Prod.* 314, 128074.
- Crini, G., and Badot, P. M. (2008). "Application of chitosan, a natural aminopolysaccharide, for dye removal from aqueous solutions by adsorption processes using batch studies: A review of recent literature," *Progress in Polymer Science* 33(4), 399-447. DOI: 10.1016/j.progpolymsci.2007.11.001
- Daiana S., Cristina P., Agustín C. and Adrián C. (2023). "Agro-industrial waste as potential heavy metal adsorbents and subsequent safe disposal of spent adsorbents. *Water* 14(20), article 3298. DOI: 10.3390/w14203298
- Deniz, F. (2024). "Cost-efficient and sustainable treatment of malachite green, a model micropollutant with a wide range of uses, from wastewater with *Pyracantha coccinea* M. J. Roemer plant, an effective and eco-friendly biosorbent," *J. Taibah University for Sci.* 18(1), article 2253592. DOI: 10.1080/16583655.2023.2253592
- Duan, C.-Y., Ma, T.-Y., Wang, J-Y., and Zhou, Y.-B. (2020). "Removal of heavy metals from aqueous solution using carbon-based adsorbents: A review," *J. Water Process Eng.* 37, article 101339. DOI: 10.1016/j.jwpe.2020.101339
- Dutta, S., Gupta, B., Srivastava, S. K., and Gupta, A. K. (2021). "Recent advances on the removal of dyes from wastewater using various adsorbents: A critical review," *Materials Advances* 2, 4497-4531. DOI: 10.1039/d1ma00354b
- Dutta, S. (2023). "Valorization of biomass-derived furfurals: reactivity patterns, synthetic strategies, and applications," *Biomass Conv. Bioref.* 13, 10361-10386. DOI: 10.1007/s13399-021-01924-w
- EL-Shimaa, I., Moustafa, H., El-molla, S. A., Shimaa, A. H., and Shaimaa, M. I. (2021). "Integrated experimental and theoretical insights for malachite green dye adsorption from wastewater using low cost adsorbent," *Water Sci. Technol.* 84 (12), 3833-3858. DOI: 10.2166/wst.2021.489
- Fernández-Sosa, E. I., Ehman, N., and Area, M. C. (2025). "Boosting the integrated use of sawmill wastes: Tannin-based extractives opportunities," *BioResources* 20(2), 2472-2475. DOI: 10.15376/biores.20.2.2472-2475
- Foo, K. Y., and Hameed, B. H. (2011). "Preparation and characterization of activated carbon from sunflower seed oil residue via microwave assisted K₂CO₃ activation," *Bioresource Technol.* 102(20), 9794-9799. DOI: 10.1016/j.biortech.2011.08.007

- Giri, B. S., Sonwani, K. R., Varjani, S., Chaurasia, D., Varadavenkatesan, T., Chaturvedi, P., Yadav, S., Katiyar, V., Singh, R. S., and Pandey, A. (2022). "Highly efficient bioadsorption of malachite green using Chinese fan-palm biochar (*Livistona chinensis*)," *Chemosphere* 287, article 132282. DOI: 10.1016/j.chemosphere.2021.132282
- Guida, M. Y., Lanaya, S., Rbihi, Z., and Hannioui A. (2019). "Thermal degradation behaviors of sawdust wood waste: pyrolysis kinetic and mechanism," *J. Mater. Environ. Sci.* 10(8), 742-755.
- Gunduz, F. and Bayrak, B. (2017). "Biosorption of malachite green from an aqueous solution using pomegranate peel: Equilibrium modelling, kinetic and thermodynamic studies," *J. Mol. Liq.* 243, 790-798.
- Gupta, V. K., and Suhas. (2009). "Application of low-cost adsorbents for dye removal A review. *Journal of Environmental Management* 90(8), 2313-2342. DOI: 10.1016/j.jenvman.2008.11.017
- Guruprasad, M. J., Rajesha, G., Shashikanth, Shareefraza J. U., Shamsuddin A., Majed A., and Saiful, I. (2024). "Studies on the removal of malachite green from its aqueous solution using water-insoluble β-cyclodextrin polymers," *ACS Omega* 9, 10132-10145. DOI: 10.1021/acsomega.3c06504
- Hasan, Z., Jeon, J., and Jhung, S. H. (2012). "Adsorptive removal of naproxen and clofibric acid from water using metal-organic frameworks," *J. Hazard Mater.* 209–210, 151-157. DOI: 10.1016/j.jhazmat.2012.01.005
- Hasanah, M., Wijaya, A., Arsyad, F. S., Mohadi, R. and Lesbani, A. (2023). "Preparation of C-based magnetic materials from fruit peel and hydrochar using snake fruit (*Salacca zalacca*) peel as adsorbents for the removal of malachite green dye," *Environ. Nat. Resour*," 21, 67-77.
- Henao-Toro, H., Juan, F. P., and Rubio-Clemente, A. (2024). "Malachite green dye removal in water by using biochar produced from *Pinus patula* pellet gasification in a reverse downdraft reactor," *Sustainability* 16(24), article 11043. DOI: 10.3390/su162411043
- Ho, Y. S., and McKay, G. (1999). "Pseudo-second order model for sorption processes," *Process Biochemistry* 34(5), 451-465. DOI: 10.1016/S0032-9592(98)00112-5
- Hubbe, M. A., Azizian, S., and Douven, S. (2019). "Implications of apparent pseudo-second-order adsorption kinetics onto cellulosic materials. A review," BioResources 14(3), 7582-7626. DOI: 10.15376/biores.14.3.7582-7626.
- Ibrahim, S. M., Hassanin, H. M., and Abdelrazek, M. M. (2020). "Synthesis, and characterization of chitosan bearing pyranoquinolinone moiety for textile dye adsorption from wastewater," *Water Sci. and Technol.* 81(3), 421-435. DOI: 10.2166/wst.2020.097
- John, O. O., Adewumi, O. D., Stephen, O. A., Robinson, O. D. and Adejoke, D. A. (2021). "Mechanism and isotherm modeling of effective adsorption of malachite green as endocrine disruptive dye using acid functionalized maize cob (AFMC)," *Scientific Reports* 11, article 21498. DOI: 10.1038/s41598-021-00993-1
- Kayode, A. A., Oreoluwa, O. A., Omolabake, A. O-A., Oyeladun, R. A., Abdullahi, B. O., Oluwaseyi, A. A, Halimat, O., Nobanathi, W. M., and Olugbenga, S. B. (2022). "Sawdust-biomass based materials for sequestration of organic and inorganic pollutants and potential for engineering applications," *Current Research in Green and Sustainable Chemistry* 5, article 100274. DOI: 10.1016/j.crgsc.2022.100274

- Khan, M. A., Khan, S., Khan, A., and Alam, M. (2017). "Soil contamination with cadmium, consequences and remediation using organic amendments," *Science of the Total Environment* 601-602, 1591-1605.
- Khan, M. U., Abas, M., Noor, S., Salah, B., Saleem, W., and Khan, R. (2021). "Experimental and statistical analysis of sawmill wood waste composite properties for practical applications," *Polymers* 13, article 4038. DOI: 10.3390/polym13224038
- Lagergren, S. (1898). "Zur Theorie der sogenannten Adsorption gelöster Stoffe," Kungliga Svenska Vetenskapsakademiens Handlingar 24(4), 1-39.
- Lata, S., Singh, P. K., and Samadder, S. R. (2015). "Regeneration of adsorbents and recovery of heavy metals: A review," *Int. J. Environ. Sci. Technol.*12, 1461-1478. DOI: 10.1007/s13762-014-0714-9
- Leila, B., Mohd, R., Abdelfateh, K., Mohammad, Q., Abeer, M. A., Hajer, S. A., and Mahmoud, A. H. A. (2022). "Review on cadmium and lead contamination: Sources, fate, mechanism, health effects and remediation methods," *Water* 14(21), article 3432. DOI: 10.3390/w14213432
- Ngeno, E. C., Mbuci, K. E., Necibi, M. C., Shikuku, V. O., Olisah, C., Ongulu, R., Matovu, H., Ssebugere, P., Abushaban, A., and Sillanpää, M. (2022). "Sustainable reutilization of waste materials as adsorbents for water and wastewater treatment in Africa: Recent studies, research gaps, and way forward for emerging economies," *Environmental Advances* 9, article 100282. DOI: 10.1016/j.envadv.2022.100282
- Ofudje, E. A., Sodiya, E., Ibadin, F. H., Ogundiran, A. A., Osideko, O. A. and Uzosike, A. (2020a). "Sorption of Cd²⁺ from aqueous solutions using cassava (*Manihot Esculenta*) waste: Equilibrium and kinetic studies," *J. Chem. Soc. Nig.* 45, 448-457.
- Ofudje, E.A., Adeogun, A.I., Idowu, M.A., Kareem, S.O., and Ndukwe, N.A. (2020b). "Simultaneous removals of cadmium (II) ions and reactive yellow 4 dye from aqueous solution by bone meal-derived apatite: kinetics, equilibrium and thermodynamic evaluations," *J. Anal. Sci. and Technol.* 11, article 7. DOI: 10.1186/s40543- 020-0206-0
- Ofudje, E. A., Sodiya, E. F., Olanrele, O. S., and Akinwunmi F. (2023). "Adsorption of Cd²⁺ onto apatitesurface: Equilibrium, kinetics and thermodynamic studies," *Heliyon* 9, article e12971. DOI: 10.1016/j.heliyon.2023.e12971
- Okpara, O. G., Ogbeide, O. M., Nworu, J. N., Chukwuekeh, J. I., Igoche, S. A., Alichi, F. S., and Orinya, O. E. (2023). "Enhanced removal of Pb(II), Cd(II), and Zn(II) ions from aqueous solutions using EDTA-synthesized activated carbon derived from sawdust," *Open Access Library Journal* 10, article e10690. DOI: 10.4236/oalib.1110690
- Qiu, B., Tao, X., Wang, H., Li, W., Ding, X., and Chu, H. (2021). "Biochar as a low-cost adsorbent for aqueous heavy metal removal: A review," *Journal of Analytical and Applied Pyrolysis* 155, article 105081. DOI: 10.1016/j.jaap.2021.105081
- Qiu, M., Liu, L., Ling, Q., Cai, Y., Yu, S., Wang, S., Fu, W., Hu, B. and Wang, X. (2022). "Biochar for the removal of contaminants from soil and water: A review," *Biochar* 4, article 19. DOI: 10.1007/s42773-022-00146-1
- Rumpa, K., Chandramoni, B., Jamil, A., Jannatul, N., and Mosummath, H.A. (2020). "A study on the adsorption of cadmium(II) from aqueous solution onto activated carbon originated from *Bombax Ceiba* fruit shell," *Journal of Chemical Health Risks* 10, 243-252.
- Sarada, B., Krishna Prasad, M., Kishore-Kumar, K., and Murthy, C. V. R. (2017). "Biosorption of Cd⁺² by green plant biomass, *Araucaria heterophylla*:

- Characterization, kinetic, isotherm and thermodynamic studies," *Appl. Water Sci.* 7, 3483-3496. DOI: 10.1007/s13201-017-0618-1
- Shanmugarajah, B., Chew, I. M., Mubarak, N. M., Choong, T. S., Yoo, C., and Tan, K. (2018). "Valorization of palm oil agro-waste into cellulose biosorbents for highly effective textile effluent remediation," *J. Cleaner Product.* 210, 697-709. DOI: 10.1016/j.jclepro.2018.10.342
- Sibel, T. A., Fatih, S., Irem, O., and Dilek, T. (2020). "A natural montmorillonite-based absorbent as an effective scavenger for cadmium contamination," *Water Air Soil Poll*. 231, article 409. DOI: 10.1007/s11270-020-04743-3
- Simon, D., Palet, C., and Cristóbal, A. (2024). "Cadmium removal by adsorption on biochars derived from wood industry and craft beer production wastes," *Water* 16, article 1905. DOI: 10.3390/w16131905
- Surjani, W., Fauziatul, F., Ridwan, J., Nazriati, N., and Endang, B. (2023). "Cadmium and lead ions adsorption on magnetite, silica, alumina, and cellulosic materials," *Sci. Rep.* 13, article 4213. DOI: 10.1038/s41598-023-30893-5
- Uzosike, A. O., Ofudje, E. A., Akiode, O. K., Ikenna, C. V., Adeogun, A. I., Akinyele, J. O., and Idowu, M. A. (2022). "Magnetic supported activated carbon obtained from walnut shells for Bisphenol-A uptake from aqueous solution," *Appl. Water Sci.* 12, article 201. DOI: 10.1007/s13201-022-01724-1
- Wang, J., Xu, W., Ren, J., Liu, X., Lu, G., and Wang, Y. (2011). "Efficient catalytic conversion of fructose into hydroxymethylfurfural by a novel carbon-based solid acid," *Green Chem.* 13, 2678-2681. DOI: 10.1039/c1gc15306d.
- Zhao, Z., Fu, D. and Ma, Q. (2014). "Adsorption characteristics of bisphenol A from aqueous solution onto HDTMAB-modified palygorskite," *Separation Science and Technology* 49(1), 81-89. DOI:10.1080/01496395.2013.818693.

Article submitted: March 27, 2025; Peer review completed: May 3, 2025; Revised version received: May 7, 2025; Accepted: June 6, 2025; Published: July 4, 2025. DOI: 10.15376/biores.20.3.7048-7074